JET PROPULSION LABORATORY   INTEROFFICE MEMORANDUM

To: MESSENGER navigation team

From: W. M. Folkner

Subject: Planetary ephemeris DE423 fit to Messenger encounters with Mercury

1. Introduction

The planetary ephemeris DE423 has been fit to estimates of the position of Mercury provided by the MESSENGER project navigation team from reconstruction of the three planetary fly-bys (normal points). Other data used previously to fit the Mercury orbit were also used in creating DE423. The addition of the MESSENGER normal points results in lower uncertainty in the Mercury orbit. The Mercury orbit uncertainty has been assessed and a covariance developed to represent the uncertainty.

The uncertainty of the Venus orbit has also been assessed at the request of the MESSENGER navigation team. The Venus orbit was fit to new range and VLBI data from the Venus Express spacecraft combined with data used for earlier ephemerides.

The orbits of the other planets are not substantially changed from the previous ephemeris DE422. The orbit of the Moon is based on the fit for DE421 and not fully converged. The lunar orbit for DE423 is consistent with the orbit on DE421 at the meter level, while the lunar libration angles are consistent at the 0.01 arcsecond level, which is adequate for many purposes. Use of DE421 is recommended for the most accurate lunar data analysis.

2. Mercury data reduction

Along with estimates of right ascension, declination and range from Earth to Mercury for each of the three MESSENGER encounters in 2008-2010, the Mercury orbit was fit to range measurements to Mariner 10 in 1974-1975, radar closure measurements from 1992-2000, and radar range data from 1965-1996.

The three MESSENGER normal points cannot be fit to their one-sigma level without changing the Earth's orbit in a way inconsistent with other, more accurate measurements. The declination from the second encounter is the least consistent single value. For fitting DE423 the declination estimate from the second encounter was de-weighted by a factor of two from the uncertainty supplied by the navigation team. Figure 1 shows the post-fit residuals for the three encounters and their nominal uncertainties.

Figure 2 shows the post-fit residuals of range from the two Mariner 10 encounters. Their residuals are comparable with fits from earlier ephemerides. Figure 3 shows the residuals for radar closure points. Their scatter is higher by about 10% than comparable residuals from DE421 that did not include any MESSENGER data, indicating that the MESSENGER data are adjusting the estimate of the Mercury orbit more strongly. Figure 4 shows the radar range residuals that are comparable with earlier ephemerides. Figure 5 shows the difference in Mercury's position between DE423 and DE421. The position change is primarily due to the addition of the MESSENGER encounter data.

3. Venus data reduction

The Venus orbit relative to Earth is now primarily determined by ranging data from the ESA Venus Express spacecraft. DE423 includes Venus Express range data from 2006 to 2009, a time span almost twice as long as used for DE421. The post-fit residuals to DE423 are shown in Figure 6. The orientation of the Earth and Venus orbits are primarily determined by VLBI measurements of spacecraft orbiting Mars, with residuals shown in Figure 7. VLBI measurements of Venus Express are now also available and along with earlier VLBI measurements from the Magellan confirm the orientation of the Venus orbit, with residuals shown in Figures 8 and 9. Residuals from estimated positions for Venus from two Cassini encounters are shown in Figure 10. Figure 11 shows the difference in positions of Venus relative to Earth between DE423 and DE421. The drift in right ascension is primarily due to the addition of more Venus Express range in DE423, and the difference in declination is mostly due to variation in the fit of Mars spacecraft VLBI data.

4. Mercury and Venus orbit uncertainties

Estimating uncertainties in planetary orbits is best done by use of independent data sets. Since there is a limited quantity of the highest precision data sets, it is often difficult to get two comparable but independent data sets. When this has been done for Mars and for Jupiter it has been found that the formal covariance from the ephemeris estimation is too optimistic by a factor of two. Since the three normal points from MESSENGER now dominate the Mercury orbit fit, it is not possible to have independent data sets with comparable accuracy. Instead, the covariance from the DE421 fit can be compared with the difference in estimated orbit between DE421 and DE423. To the extent that the DE423 orbit is dominated by the MESSENGER data, the difference in Mercury orbits between DE421 and DE423 should be comparable with the formal uncertainty from the DE421 fit, which is higher than the uncertainty for DE423.

Figure 12 shows the formal uncertainty in the Mercury orbit from the DE421 fit scaled up by two as found appropriate from the Mars and Jupiter studies. This uncertainty is assessed to be comparable with the difference in Mercury orbit between DE421 and DE423 (Figure 5). Thus it is expected that twice the formal uncertainty in the DE423 fit should be a reasonable representation of the realistic one-sigma Mercury orbit uncertainty. However this relies on the MESSENGER encounter data for which there are not enough points to independently assess. Since the DE423 uncertainty, which is based on the MESSENGER encounter data, is less than twice the uncertainty from DE421 without the MESSENGER data, the normal navigation process of planning for up to a 3-sigma error should be reasonable using twice the DE423 uncertainty and the realistic 1-sigma uncertainty.

Similarly for Venus, the difference in estimated orbit between DE421 and DE423 shown in Figure 11 is expected to be about twice the formal uncertainty from the DE421 fit, since DE423 includes twice as much Venus Express range data and has a variation of orbit orientation from fitting Mars spacecraft VLBI data. Figure 14 shows twice the formal uncertainty in the DE421 fit. Figure 15 shows twice the formal uncertainty in the DE423 fit, which is smaller than the uncertainty from the DE421 fit and is expected to represent the realistic uncertainty for DE423.

The estimated orbital uncertainties described above are based on the data weighting used in the fits and include correlations between all the planetary orbital elements and with a number of other estimated parameters. For the use by the MESSENGER navigation team, a covariance matrix for just the 18 orbital element parameters for Mercury, Venus, and the Earth-Moon

barycenter (EMB) was constructed to approximate the scaled orbital uncertainty from the DE423 fit. The covariance matrix representing the realistic one-sigma uncertainty in units of radian^2 with orbital elements in the Set-III from (Brouwer & Clemence 1961) is given below. Figure 16 shows the uncertainty in the Mercury orbit from this covariance matrix, and Figure 17 shows the uncertainty in the Venus orbit. The Venus orbit uncertainty in right ascension from the 18 element covariance is larger than from the formal DE423 covariance. With only the 18 orbital elements in use a smaller right ascension uncertainty would results in a range uncertainty lower than the formal covariance, which is not realistic.

References

D. Brouwer and G. M. Clemence, Methods of celestial mechanics, Academic Press, New York, 1961.

W. M. Folkner, J. G. Williams, and D. H. Boggs, The planetary ephemeris DE421, JPL IPN Progress Reports, v. 42-178, http://ipnpr.jpl.nasa.gov/index.cfm, August 2009.

W. M. Folkner, Uncertainty in the orbits of Earth and Mars for MSL planning, JPL IOM 343R-06-003, 25 April 2006.

Moyer, T. D. 2000. *Formulation for Observed and Computed Values of Deep Space Network Data Types for Navigation.* DESCANSO Monograph 2. JPL Publication 00-7. Jet Propulsion Laboratory, California Institute of Technology, Pasadena, CA, http://descanso.jpl.nasa.gov/Monograph/series2/Descanso2_all.pdf.

Acknowledgements

Cc:

JPL Solar System Dynamics Group

Covariance matrix representing the uncertainty in the orbits of Mercury, Venus, and the Earth-Moon barycenter for ephemeris DE423. The covariance is expressed in Set III orbital element corrections, in units of radians^2.

```
APCSCALE1 =  18*1.D0
APCNAME1(1) =
'DMW1   ','DP1    ','DQ1    ','EDW1   ','DA1    ','DE1    ',
'DMW2   ','DP2    ','DQ2    ','EDW2   ','DA2    ','DE2    ',
'DMWB   ','DPB    ','DQB    ','EDWB   ','DAB    ','DEB    ',
APCOV1( 1, 1) =   1.146082406510E-17,
APCOV1( 1, 2) =  -7.311797494451E-18,  1.748816574697E-16,
APCOV1( 1, 3) =  -3.081734955449E-19, -2.023261181281E-17,  1.603182359173E-16,
APCOV1( 1, 4) =  -1.404918557080E-18,  2.721191548966E-18, -3.354727675562E-18,
                  1.326973918182E-18,
APCOV1( 1, 5) =   8.913162049848E-21, -3.367167575422E-21,  8.377313816629E-21,
                 -2.358099137280E-21,  1.008848340642E-23,
APCOV1( 1, 6) =  -4.812336429748E-19,  4.425611017940E-18, -5.125429242682E-18,
                  2.678707427459E-19, -1.130357100701E-21,  1.245085632124E-18,
APCOV1( 1, 7) =   1.579869209542E-18,  7.307679819829E-19,  1.160717590388E-18,
                  2.730414891847E-19,  3.369522086340E-22, -4.465330158709E-20,
                  1.696019408476E-18,
APCOV1( 1, 8) =  -7.844180618174E-19,  6.700732882345E-18,  9.564795412578E-18,
                 -1.158573806862E-19,  7.701306231359E-23, -7.001242396440E-20,
                 -7.975780652186E-20,  6.004920031797E-18,
APCOV1( 1, 9) =  -9.899365925962E-20, -3.450998520931E-18,  4.518898073142E-19,
                  2.428742116915E-20, -1.684568507934E-22,  9.868414740039E-20,
                 -1.821510550329E-19,  1.032911260322E-18,  4.581662575713E-18,
APCOV1( 1,10) =   6.364833957026E-21,  6.363244204235E-21,  1.008898889364E-20,
                  1.626982964632E-21, -1.080606986118E-24, -4.960060902581E-22,
                  7.091585023461E-21, -2.246345160777E-22, -1.005456336976E-21,
                  1.178077741720E-22,
APCOV1( 1,11) =   1.035947795860E-21, -4.059815678416E-22, -4.570593433163E-22,
                  5.848279801407E-23,  8.272590735946E-25,  3.462732801954E-23,
                  1.053922874166E-21, -9.169109852614E-23, -6.742753370884E-23,
                 -3.312483830484E-24,  2.561224573175E-24,
APCOV1( 1,12) =  -3.590013604675E-23, -1.571436404363E-22,  7.033887677988E-22,
                  5.447359268447E-23, -5.922624472174E-26,  4.201478183975E-23,
                  2.054038507612E-22,  6.215837925169E-23,  5.534036487128E-23,
                 -7.542464151900E-25,  2.036254559880E-25,  5.192287982290E-23,
APCOV1( 1,13) =   1.552819193401E-18,  9.323351648229E-19,  1.638237272302E-18,
                  2.688364425354E-19,  3.469377319440E-22, -4.406668452108E-20,
                  1.674548881616E-18,  2.444947228311E-19,  2.281371544200E-20,
                  6.986458478077E-21,  1.041008790265E-21, -3.007901320634E-23,
                  1.702528512726E-18,
APCOV1( 1,14) =  -6.640067102854E-19,  7.509543146440E-18,  8.120433427680E-18,
                 -1.190823189352E-19,  1.522777948675E-22, -1.068657839692E-19,
                 -9.420660737801E-21,  4.754249223919E-18, -1.298629980470E-18,
                  6.783537069055E-23, -3.659962331990E-23,  4.033479178489E-23,
                  1.763188610868E-19,  4.789785390396E-18,
APCOV1( 1,15) =  -5.199978789132E-19,  1.477789031393E-19,  4.914523550038E-18,
                 -4.725558677399E-20, -1.072553247355E-22,  5.605037957617E-20,
                 -2.616607198079E-19,  3.777720941832E-18,  4.506184711954E-18,
                 -1.483285403469E-21, -9.703826605516E-23,  5.934369684449E-23,
                  7.575176988396E-20,  1.144082062156E-18,  5.770258341380E-18,
APCOV1( 1,16) =   1.551162976240E-20,  1.949337830722E-20,  3.179688239871E-20,
                  3.945521275593E-21, -2.470584493035E-24, -1.108589642323E-21,
                  1.791777111493E-20,  4.963514069128E-21,  1.078546498994E-21,
                  1.887041887104E-22, -7.295960822478E-24,  1.678708880685E-23,
                  1.793459833388E-20,  3.259135870709E-21,  2.155979722819E-21,
                  4.134734417155E-22,
APCOV1( 1,17) =   1.704622714136E-21, -6.986056353797E-22, -7.732452353497E-22,
                  9.845392547550E-23,  1.365021459139E-24,  5.949022988052E-23,
                  1.668200641961E-21, -1.574037989869E-22, -1.127819309858E-22,
                 -5.602355208444E-24,  4.136340766940E-24, -3.165604888078E-25,
                  1.720861372926E-21, -6.334513843588E-23, -1.569290427911E-22,
                 -1.270745153400E-23,  6.884776429904E-24,
APCOV1( 1,18) =  -2.739537965148E-22,  1.389283584514E-22,  2.983128710078E-22,
                  3.971301444274E-23, -3.081110287253E-25,  5.083355467466E-23,
                  2.312568015837E-23, -2.702004184151E-23,  4.281733283716E-23,
                 -1.709410346682E-23, -3.897701118470E-25,  3.878178535798E-23,
                 -2.758336615628E-22,  4.565359280669E-23,  8.936535135364E-25,
                  2.430983299351E-24, -1.450174183977E-24,  4.530870217046E-23,
```
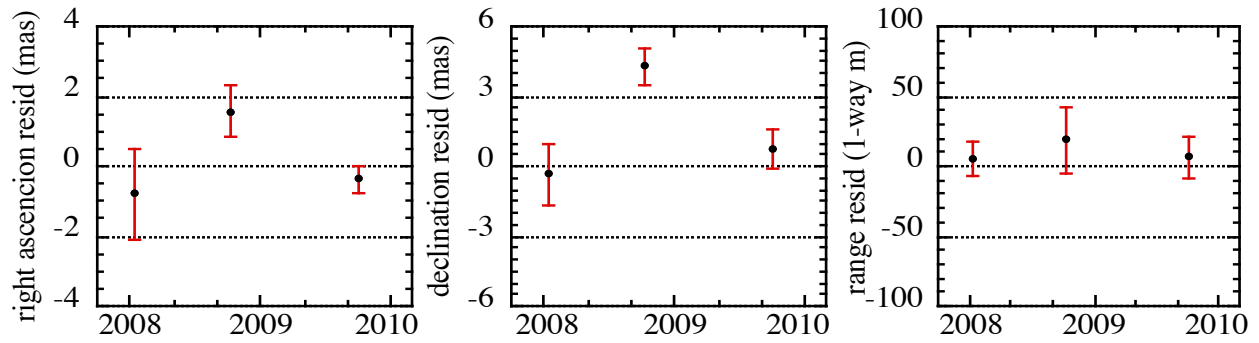
Figure 1: Residuals of estimated positions of Mercury from the MESSENGER encounters.
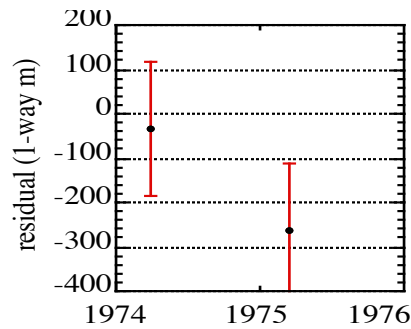
Figure 2: Residuals of estimated range to Mercury from the Mariner 10 encounters.
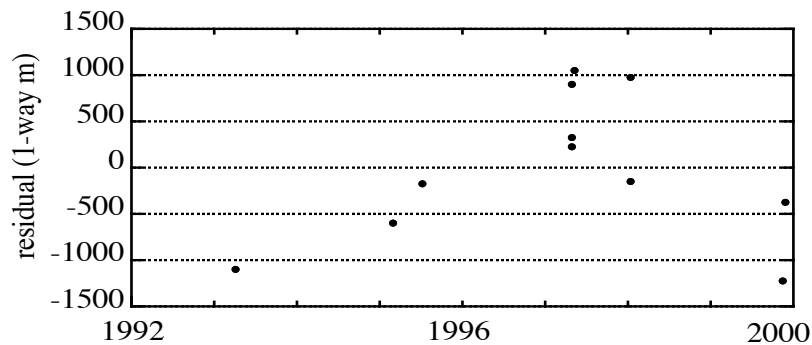
Figure 3: Residuals of Mercury radar closure measurements.
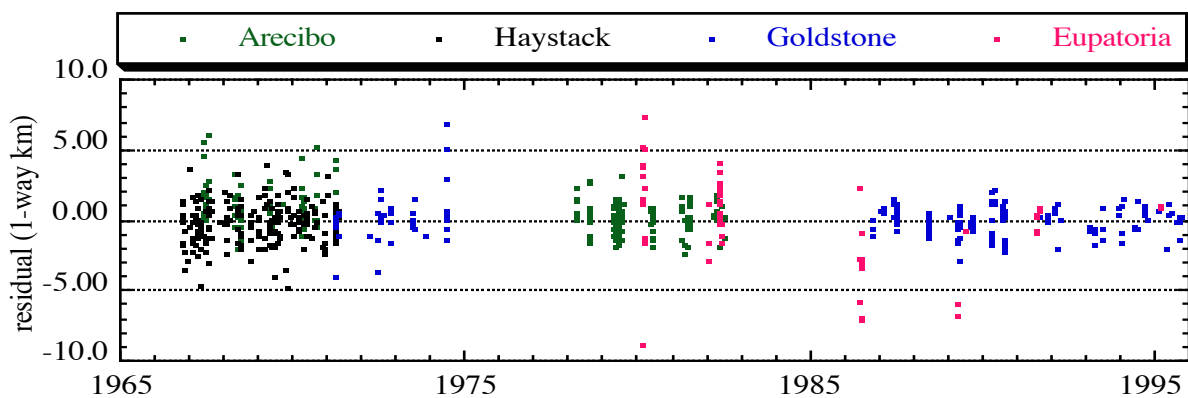
Figure 4: Residuals of Mercury radar range measurements.

R.A. : 423−421, Mercury − Earth

Dec. : 423−421, Mercury − Earth

Dist : 423−421, Mercury − Earth
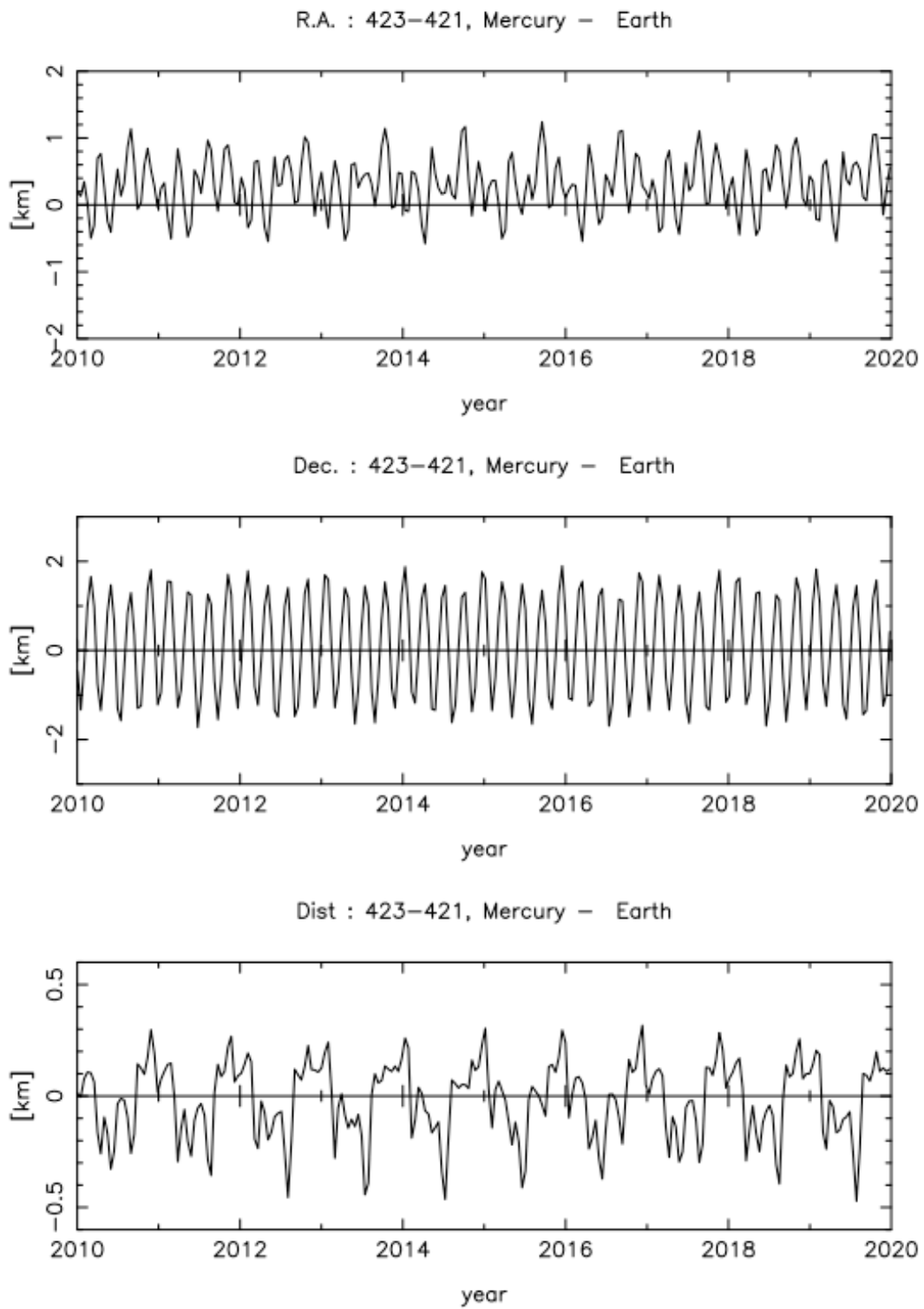
Figure 5: Difference in position of Mercury relative to Earth between ephemerides DE421 and DE423.
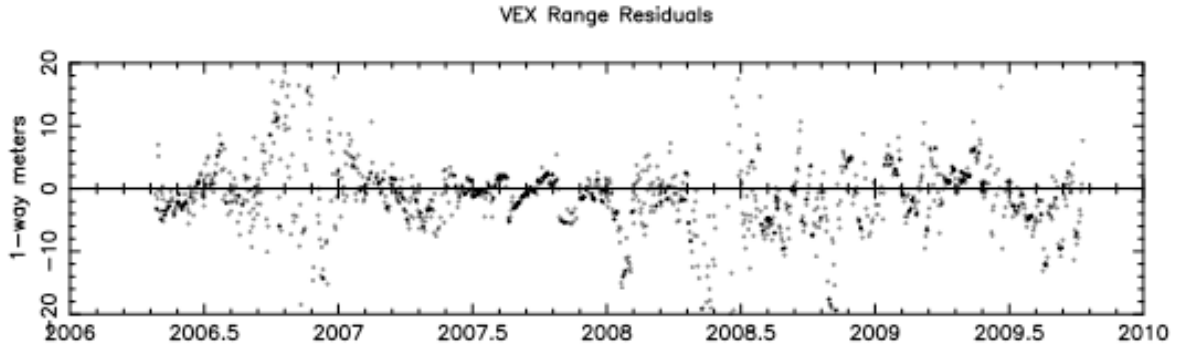
Figure 6: Venus Express range residuals against ephemeris DE423.
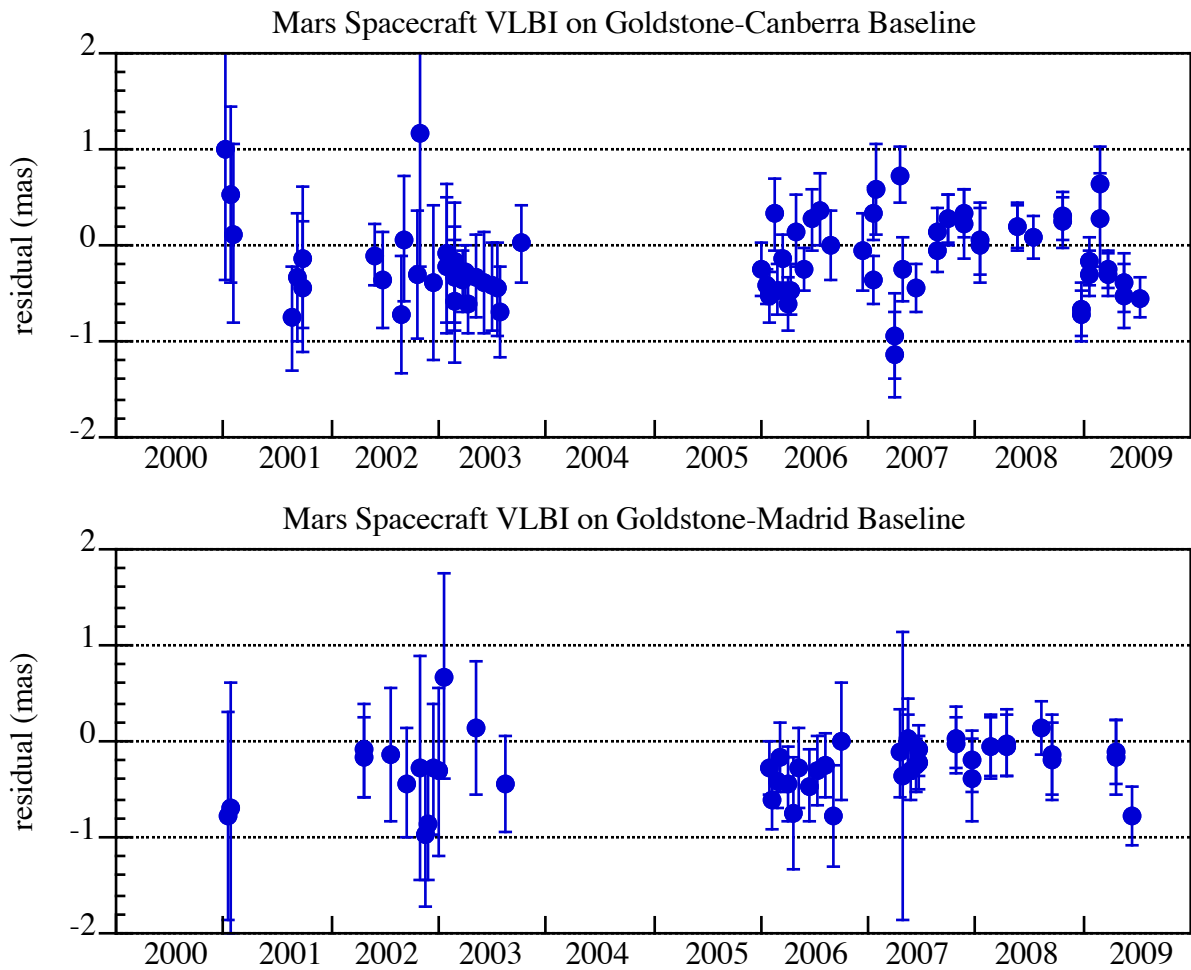
Figure 7: Mars spacecraft VLBI residuals against ephemeris DE423.
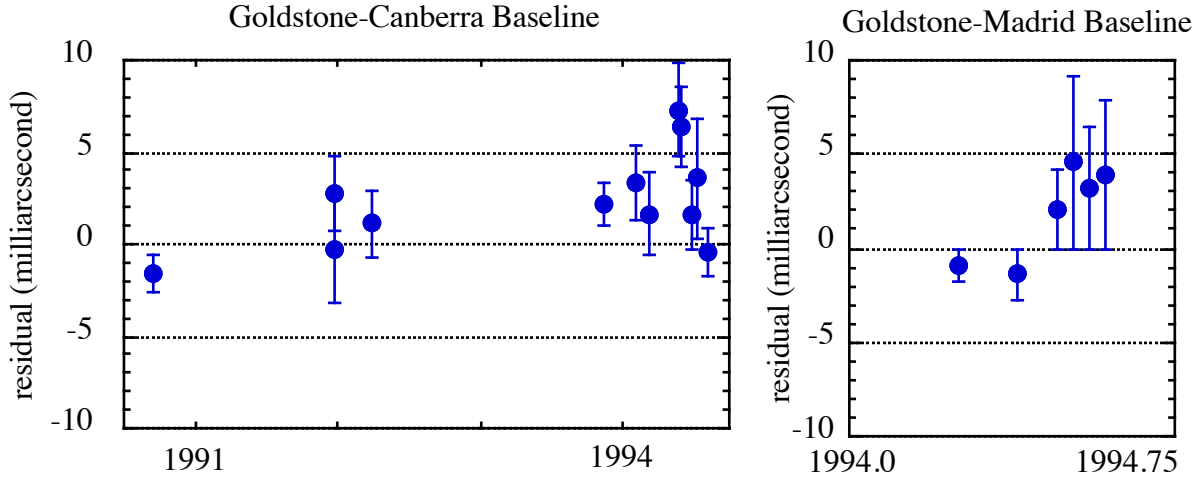
Figure 8: Magellan VLBI residuals against ephemeris DE423.
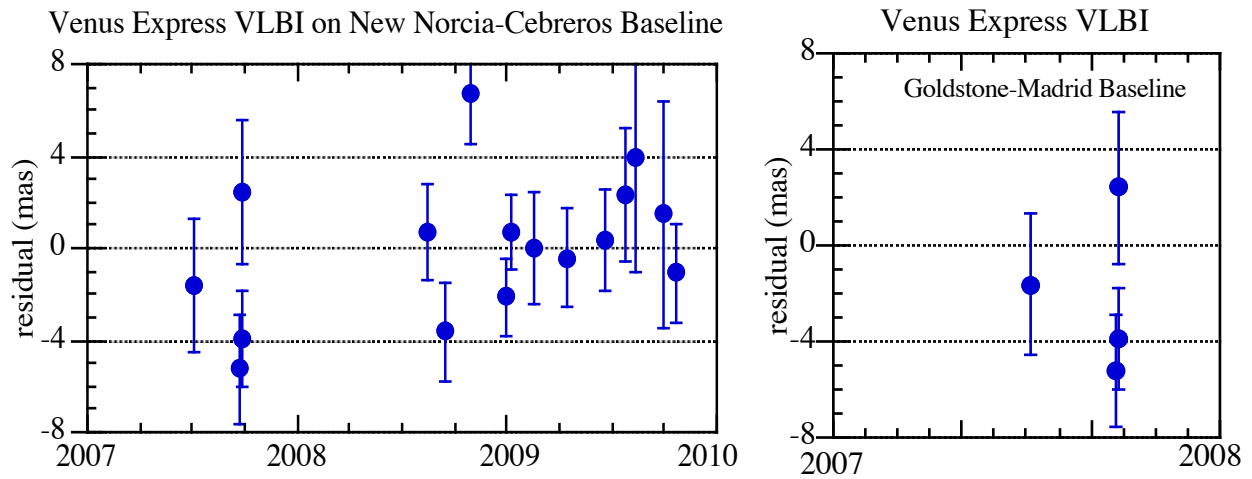
Figure 9: Venus Express VLBI residuals against ephemeris DE423.
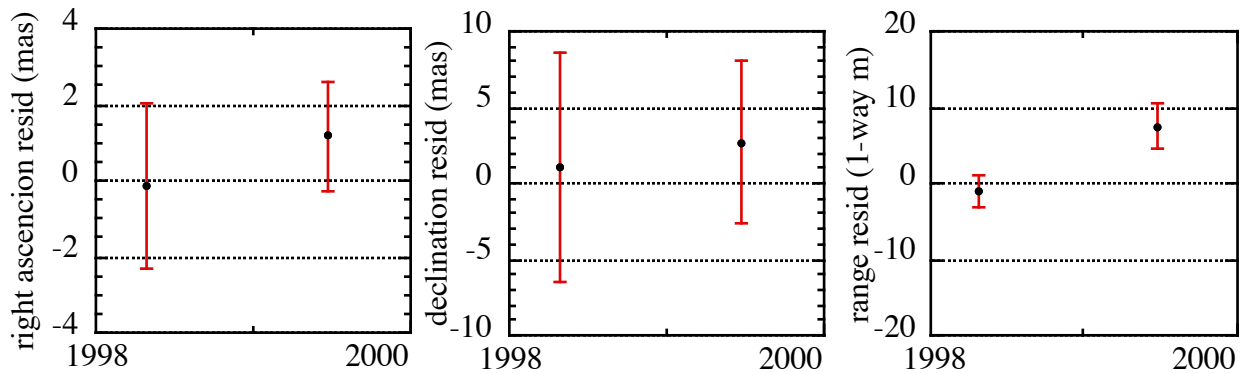
Figure 10: Venus position residuals from Cassini encounters against ephemeris DE423.

R.A. : 423−421,   Venus − Earth

Dec. : 423−421,   Venus − Earth

Dist : 423−421,   Venus − Earth
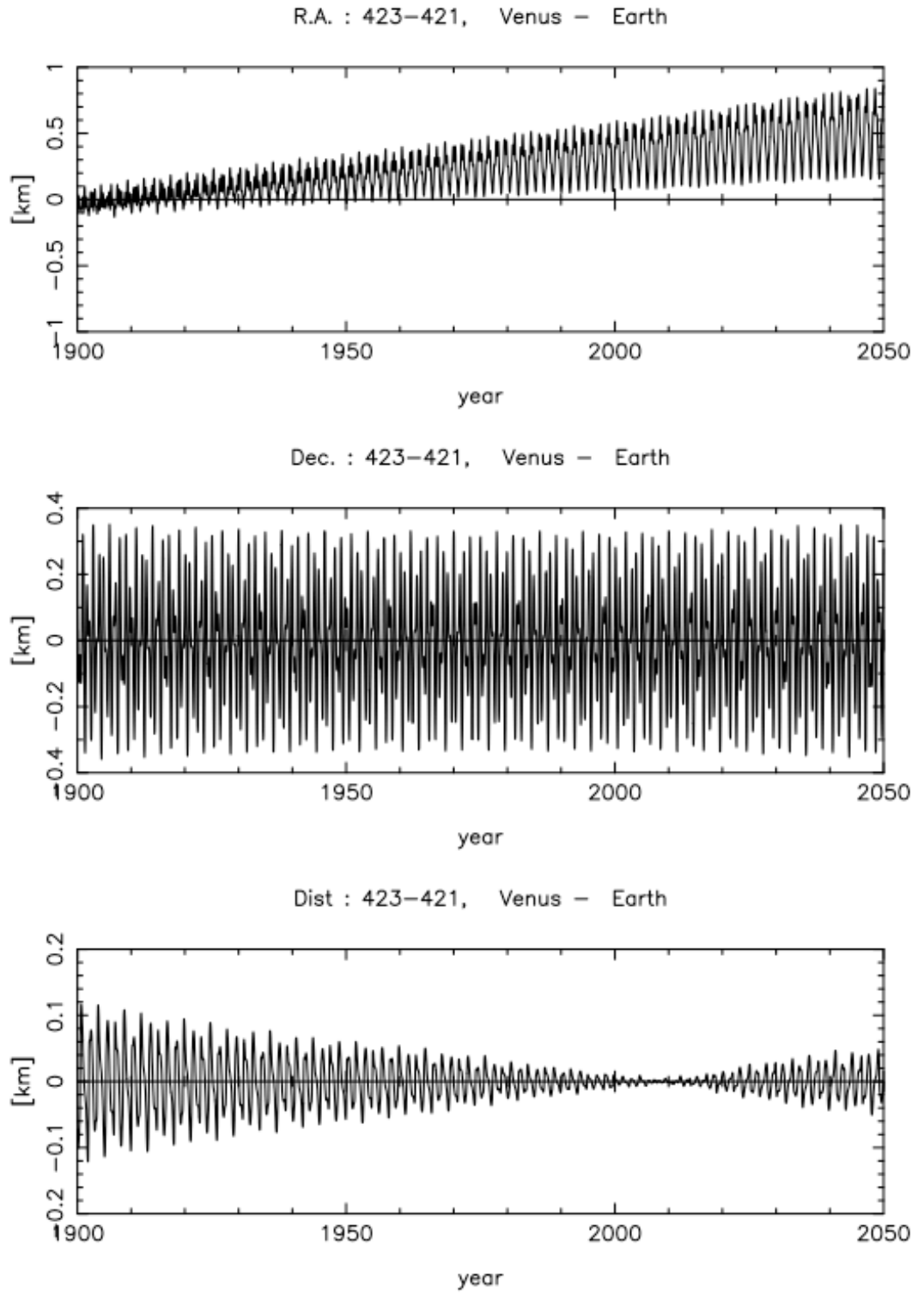
Figure 11: Difference in position of Venus relative to Earth between ephemerides DE423 and DE421.

9
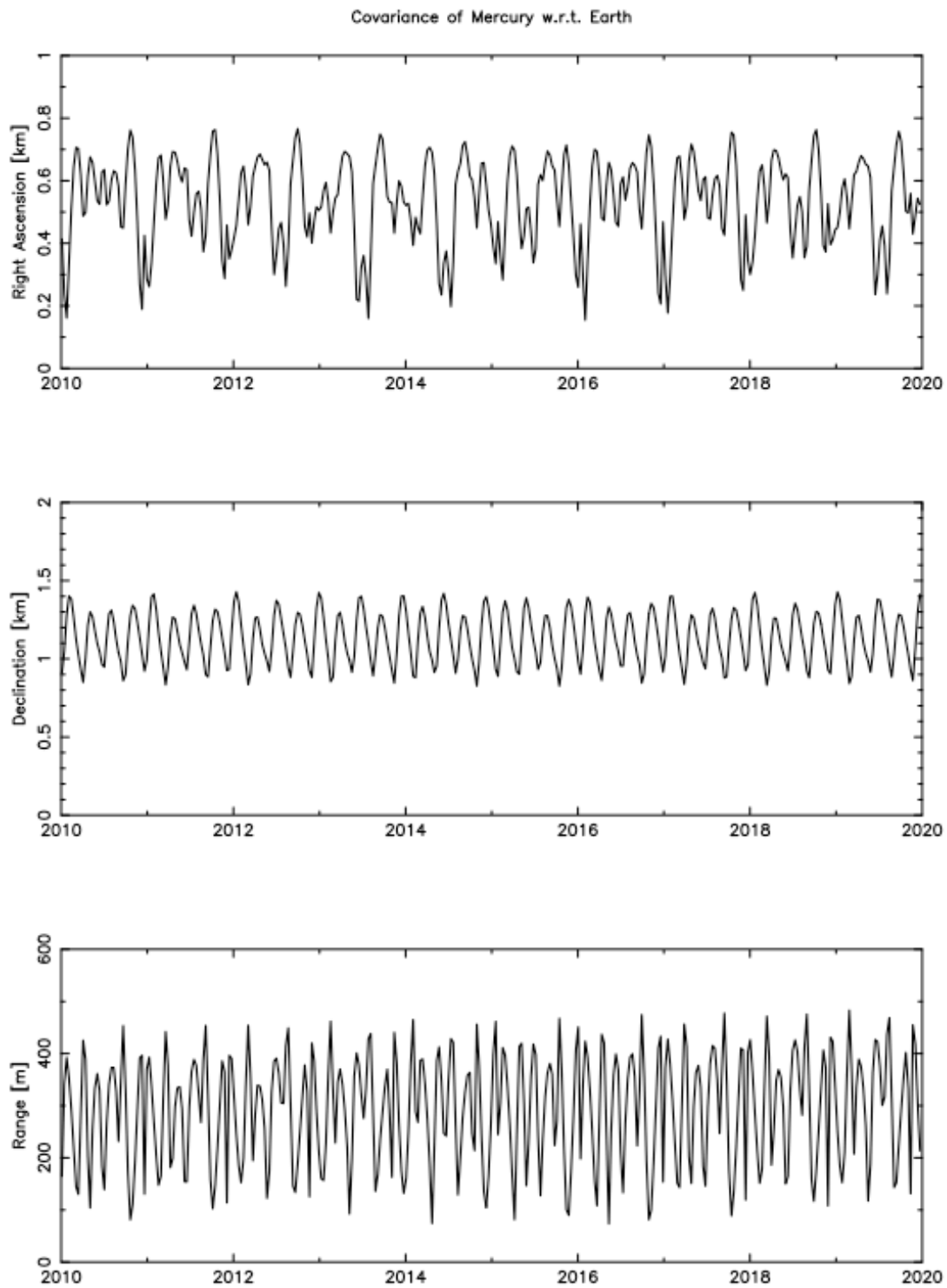
Figure 12: Twice the formal uncertainty in the orbit of Mercury relative to Earth from the DE421 ephemeris.

Covariance of Mercury w.r.t. Earth
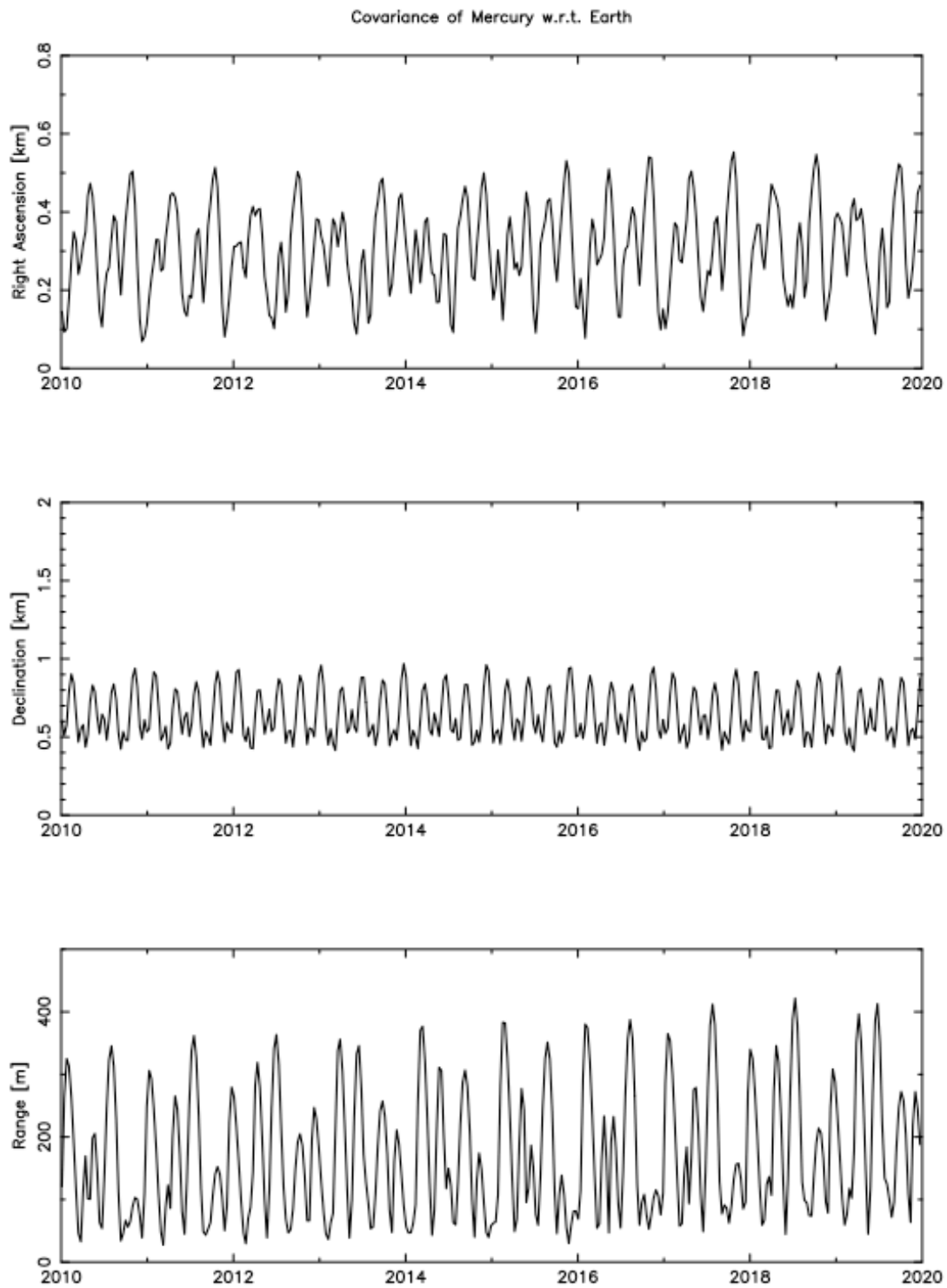
Figure 13: Twice the formal uncertainty in the orbit of Mercury relative to Earth from the DE423 ephemeris.
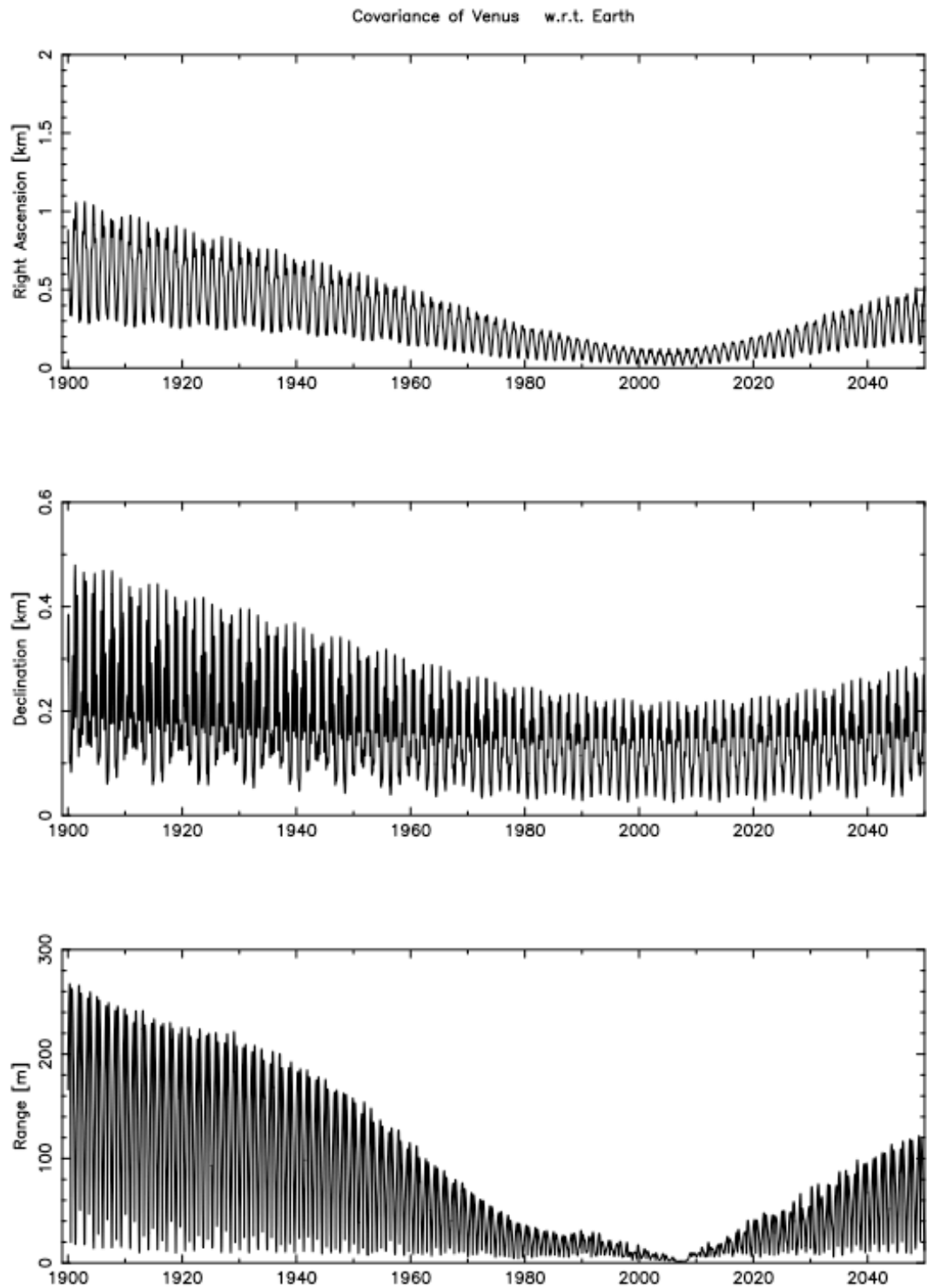
Figure 14: Twice the formal uncertainty in the orbit of Venus relative to Earth from the DE421 ephemeris.

Covariance of Venus   w.r.t. Earth
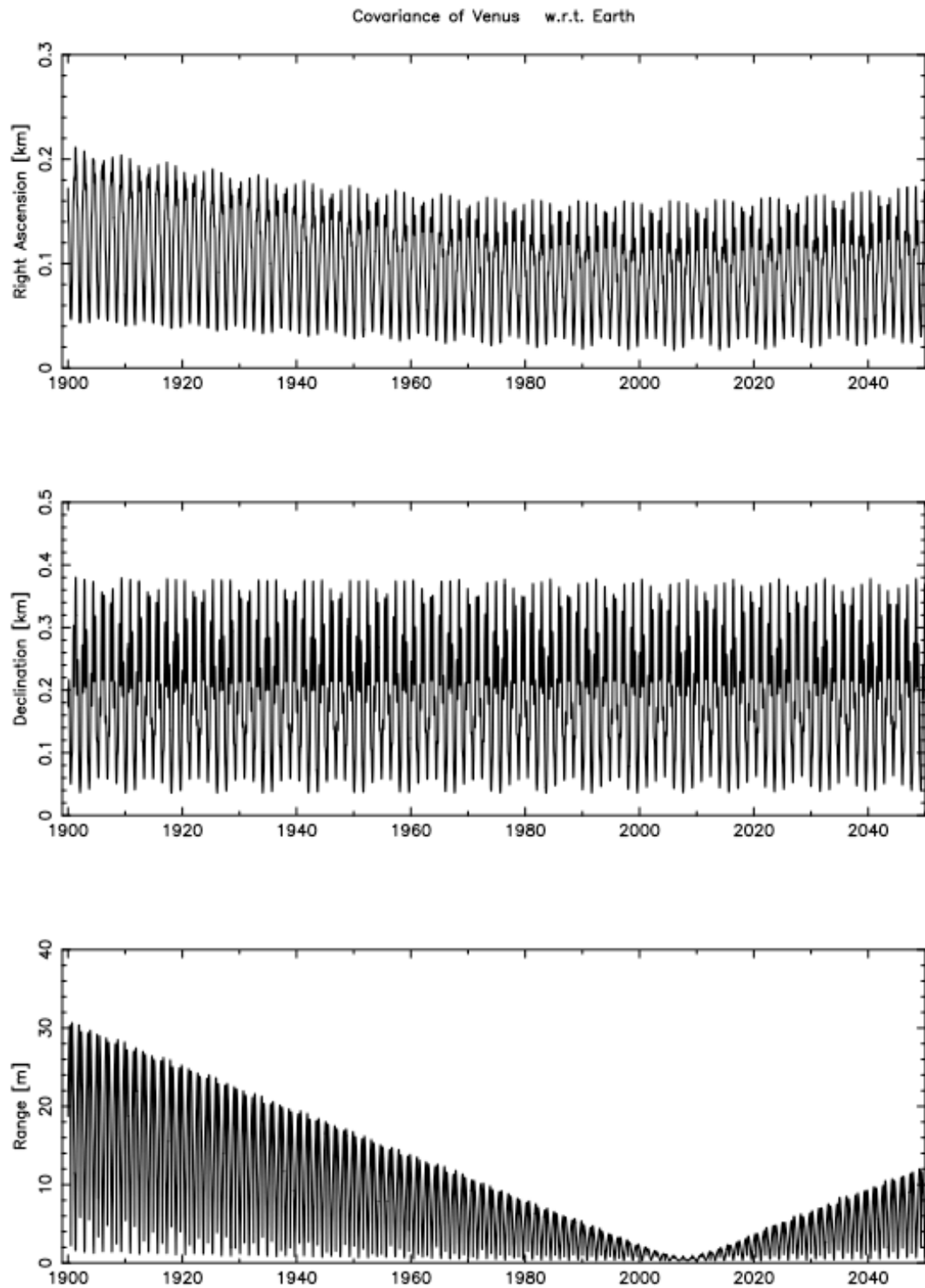
Figure 15: Twice the formal uncertainty in the orbit of Venus relative to Earth from the DE423 ephemeris.

Covariance of Mercury w.r.t. Earth
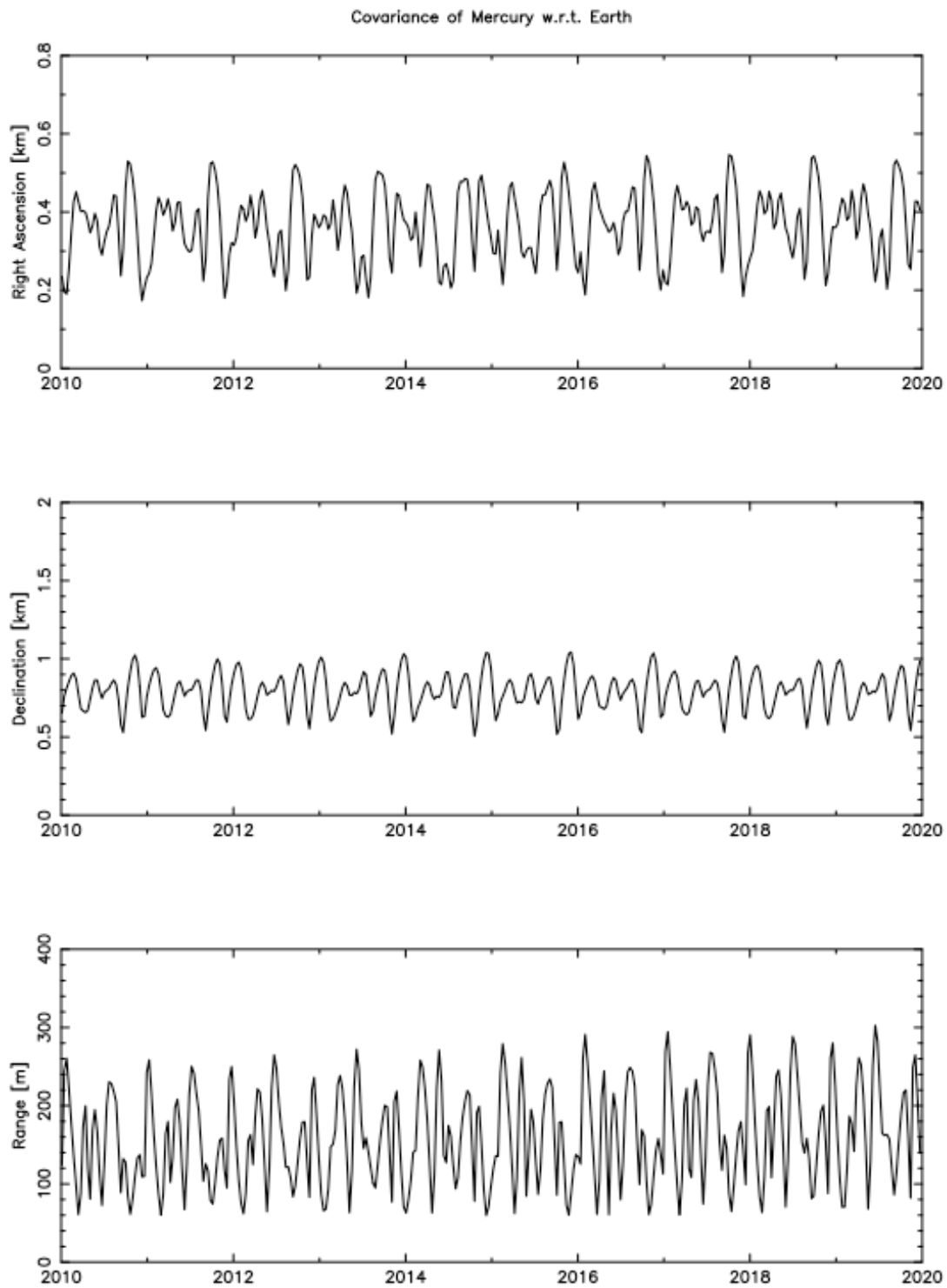
Figure 16: Realistic one-sigma uncertainty in the orbit of Mercury relative to Earth from the 18-element covariance for Mercury, Venus, and Earth-Moon barycenter.

Covariance of Venus   w.r.t. Earth
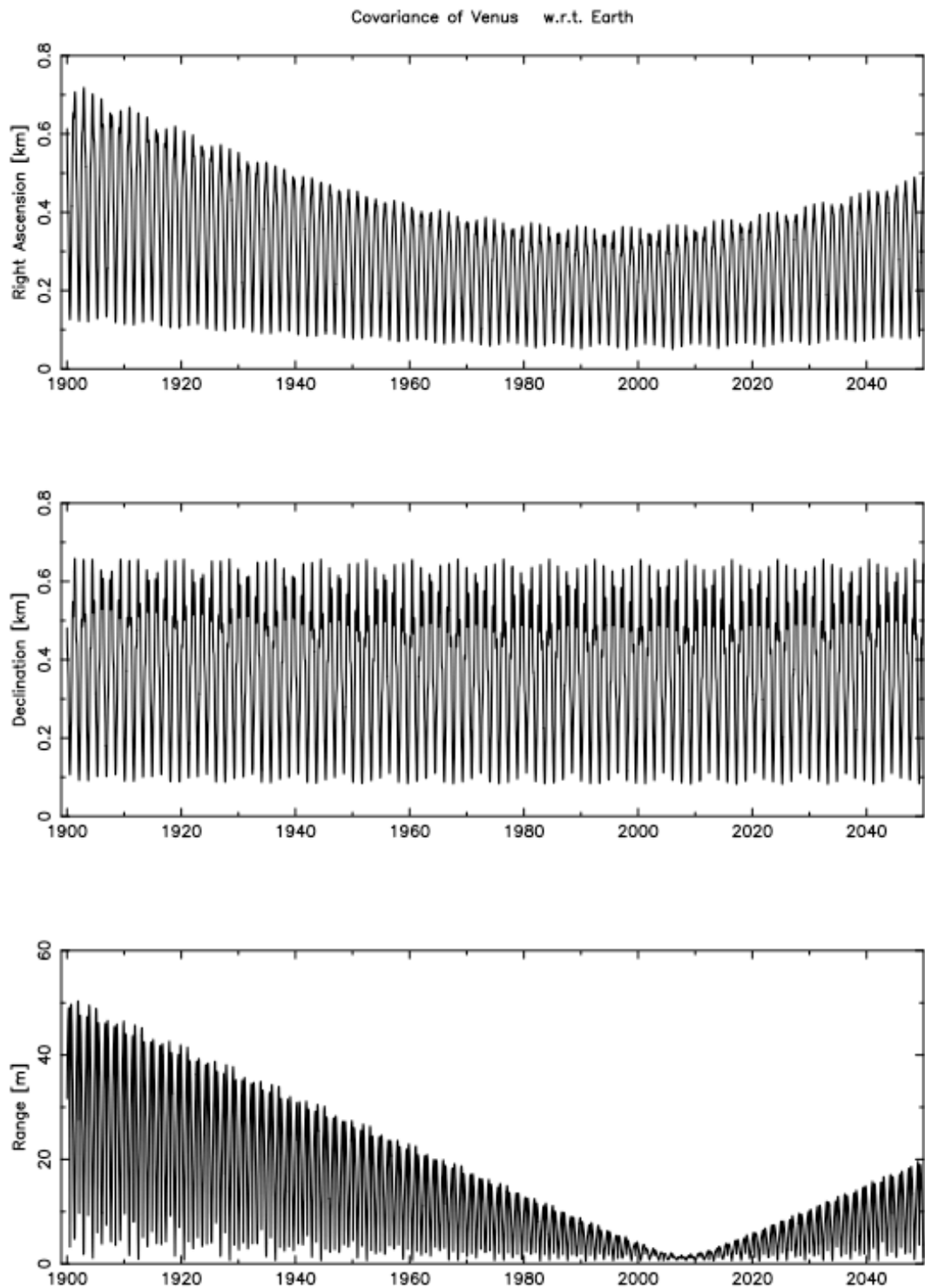
Figure 17: Realistic one-sigma uncertainty in the orbit of Venus relative to Earth from the 18-element covariance for Mercury, Venus, and Earth-Moon barycenter.